OrgXenomics: an integrated proteomic knowledge base for patient-derived organoid and xenograft

Yintao Zhang [1,2,†], Xichen Lian[1,†], Hangwei Xu[1,†], Sisi Zhu[3], Hao Zhang[3], Ziheng Ni[3], Tingting Fu[1], Shuiping Liu [3], Lin Tao [3,*], Ying Zhou[1,*] and Feng Zhu [1,2,*]

[1]College of Pharmaceutical Sciences, Department of Pharmacy, Second Affiliated Hospital, Zhejiang University School of Medicine, State Key Laboratory of Advanced Drug Delivery and Release Systems, Zhejiang University, Hangzhou 310058, China
[2]Innovation Institute for Artificial Intelligence in Medicine of Zhejiang University, Alibaba-Zhejiang University Joint Research Center of Future Digital Healthcare, Hangzhou 330110, China
[3]Key Laboratory of Elemene Class Anti-Cancer Chinese Medicines, School of Pharmacy, Hangzhou Normal University, Hangzhou 311121, China

*To whom correspondence should be addressed. Tel: +86 189 8946 6518; Email: zhufeng@zju.edu.cn
Correspondence may also be addressed to Prof. Ying Zhou. Email: zhou_ying@zju.edu.cn
Correspondence may also be addressed to Prof. Lin Tao. Email: taolin@hznu.edu.cn
†The first three authors should be regarded as Joint First Authors.

Abstract

Patient-derived models (PDMs, particularly organoids and xenografts) are irreplaceable tools for precision medicine, from target development to lead identification, then to preclinical evaluation, and finally to clinical decision-making. So far, PDM-based proteomics has emerged to be one of the cutting-edge directions and massive data have been accumulated. However, such PDM-based proteomic data have not been provided by any of the available databases, and proteomics profiles of all proteins in proteomic study are also completely absent from existing databases. Herein, an integrated database named '*OrgXenomics*' was thus developed to provide the proteomic data for PDMs, which was unique in (a) explicitly describing the establishment detail for a wide array of models, (b) systematically providing the proteomic profiles (expression/function/interaction) for all proteins in studied proteomic analysis and (c) comprehensively giving the raw data for diverse organoid/xenograft-based proteomic studies of various diseases. Our *OrgXenomics* was expected to server as one good complement to existing proteomic databases, and had great implication for the practice of precision medicine, which could be accessed at: https://idrblab.org/orgxenomics/

Graphical abstract
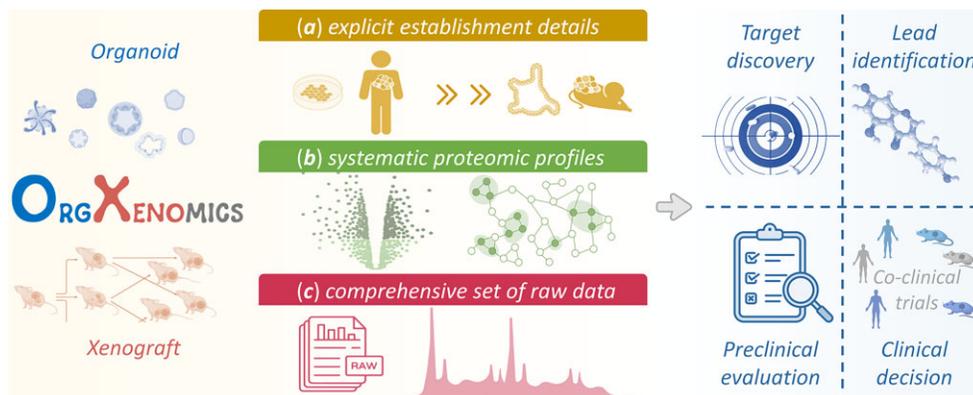
Introduction

Patient-derived models (PDMs, particularly organoids and xenografts) are irreplaceable tools for precision medicine, from target development to lead identification, then to preclinical evaluation, and finally to clinical decision-making (1). In comparison to cell line models, PDMs are reported to be more accurate in capturing the pathophysiological features of disease development and key for bridging the translational gaps from laboratory ideas to clinical applications (2–4). So far, the PDM-based proteomics has become one of the cutting-edge fields (5–7), which fosters significant advancement in identifying therapeutic target (8–10), predicting drug response

(11–13), revealing resistance mechanism (14–17), etc. With the advance in model establishment protocol, the PDM-based proteomics data have seen a rapid accumulation, which provides invaluable foundation for the application of AI (18–20) to promote the modern practice of precision medicine (21–24).

Till now, several proteomic databases have been constructed, including *PRIDE* (25), *jPOST* (26), *MassIVE* (27), *iProX* (28) and *ProteomeXchange* (29). As provided in Table 1, although all these repositories diligently curate raw data for diverse proteomic analyses, none of them specialize in describing PDM-based proteomic data. Moreover, the detailed proteomic profiles of each OMIC study were largely absent from existing databases. Such valuable profiles include the expressions, functions and interactions of each protein in the corresponding study. In other words, a proteomic database offering PDM (especially organoid and xenograft) data is therefore highly demanded.

In this study, an integrated database 'OrgXenomics' was thus developed to provide the proteomic data for PDMs. Particularly, our *OrgXenomics* contained 399 datasets relevant to patient-derived models (including 267 organoid datasets and 132 xenograft datasets). Furthermore, each proteomic dataset was curated to retrieve detailed proteomic information, such as PDM type (PDX for liver cancer, PDO for pancreatic cancer, etc.), disease (ulcerative colitis, breast cancer, SARS-CoV-2, scleroderma, etc.), tissue source (bone marrow, colonic biopsy, etc.), and culture protocols. These datasets covered 23 tissue origins and 45 disease classes. Additionally, the proteomic profiles for each dataset were thoroughly analyzed and visualized in our database, and a variety of interactive plots were generated online to illustrate their differential expression patterns, enriched functional insights and molecular interactions for all proteins expressed in each proteomic study.

All in all, our *OrgXenomics* database (shown in Figure 1) was unique in (a) explicitly describing the establishment detail for a wide array of tissue/organ models, (b) systematically providing the proteomic profiles (expression/function/interaction) for all proteins in each proteomic study and (c) comprehensively giving the raw data for diverse organoid/xenograft-based proteomic studies of various diseases. Moreover, the proteins, pathways, species and diseases in *OrgXenomics* were cross-linked to several established databases, including but not limited to UniProt (30), PDB (31), AlphaFold DB (32), TTD (33), NCBI Taxonomy (34), RefSeq (35), Ensembl (36), VARIDT (37), KEGG (38), Reactome (39), Gene Ontology (40), WHO ICD (41), TheMarker (42), HGNC (43) and INTEDE (44). Our *OrgXenomics* is expected to server as an essential complement to existing proteomic and PDM transcriptomic databases (45) in facilitating precision medicine study.

Factual content and data retrieval

Systematic collection and curation of the PDM-based proteomics datasets

The proteomic datasets of patient-derived model offered in *OrgXenomics* were collected through the meticulous procedures. First, comprehensive literature review was conducted using keyword combination 'organoid + proteomics', 'xenograft + proteomics', 'PDX + proteomics' in PubMed (46) and several existing databases such as PRIDE. Sec-

ond, all those identified publications were manually scrutinized based on the following criteria for data exclusions, including: (a) proteomic studies that were not conducted on organoids/xenografts and (b) proteomic studies that provided neither raw data nor the expression matrix. As a result, a total of 399 PDM proteomic datasets of organoid/xenograft were collected. Third, the detailed information for each dataset was carefully extracted from the corresponding study, such as PDM type, tissue sources, and disease indication. Additionally, the detailed protocol for model culture was also documented in explicit detail.

In *OrgXenomics*, the general information for each project was systematically presented as shown in Figure 2. Standardized information collected for the organoid and xenograft proteomic project included *title*, *studied diseases*, *organism*, *quantification methods* and *instrument*. Moreover, for organoid proteomic projects, additional information such as *organoid type*, *organoid source* and *culture protocols* were also recorded. For xenograft proteomic projects, invaluable data including *xenograft source*, *implanted species* and *implanted locations* were clearly documented.

Standard pipeline for data processing and differential expression analysis

The raw data of the collected proteomics datasets were downloaded from the data repositories in which they were stored and processed using the following procedures. First, the raw data of each dataset were quantified by *MaxQuant* (v2.4.0.0) (47), and the applied quantification method and experimental designs (such as *parameter group*, *experiment* and *fraction*) were set according to the parameters in the original publication. Second, the protein sequences (in FASTA format) from the same species as that of the original publication were collected from the *UniProt* and evaluated using the *MaxQuant* to facilitate the subsequent annotations of the identified peptide peaks. Third, the detailed search parameters were configured based on the original publication, which included the modification (both fixed and variable), digestion mode, mass tolerance, threshold of peptide's false discovery rates, and so on. When the explicit search parameters were not made available in the corresponding original publication, the default settings in *MaxQuant* were employed.

The output file *proteinGroups.txt* generated by *MaxQuant* was subjected to further analysis using *Perseus* (48) to gain biological insights. In particular, the proteins matching to *MaxQuant*'s built-in databases (contaminants and reverse protein sequences) were *first* excluded from our analyses. *Second*, the raw intensities were normalized based on *log-transformation* to deal with the skewed distribution of protein intensities and to make the data more suitable for statistical analyses. *Third*, the threshold for missing data across samples was set to 30%, and the imputation of missing data was carried out using the sample-wise approach with a width of 0.3 standard deviations (SD) and a downshift of 1.8 SD, which was used to approximate the distribution of low-abundance protein that was below the detection limit. Fourth, based on the resulting intensity data, the permutation-based false discovery rate measurement was used to enable multiple hypothesis testing correction, and the processed data were evaluated based on multiple criteria proposed in previous study (49). For the datasets having a large fraction of missing value or demonstrating severe systematic bias, additional processing

Table 1. Comparing the key database features of our *OrgXenomics* with that of existing proteomic databases

| Key database features	OrgXenomics	PRIDE	jPOST	MassIVE	iProX	ProteomicsDB	RiceProteomeDB
Data analysis							
Expression profile	√	×	×	×	×	×	×
Function profile	√	×	×	×	×	×	×
Interaction profile	√	×	×	×	×	×	×
Raw data download	√	√	√	√	√	×	×
Multiple species	√	√	√	√	√	√	×
Specific for PDM	√	×	×	×	×	×	×
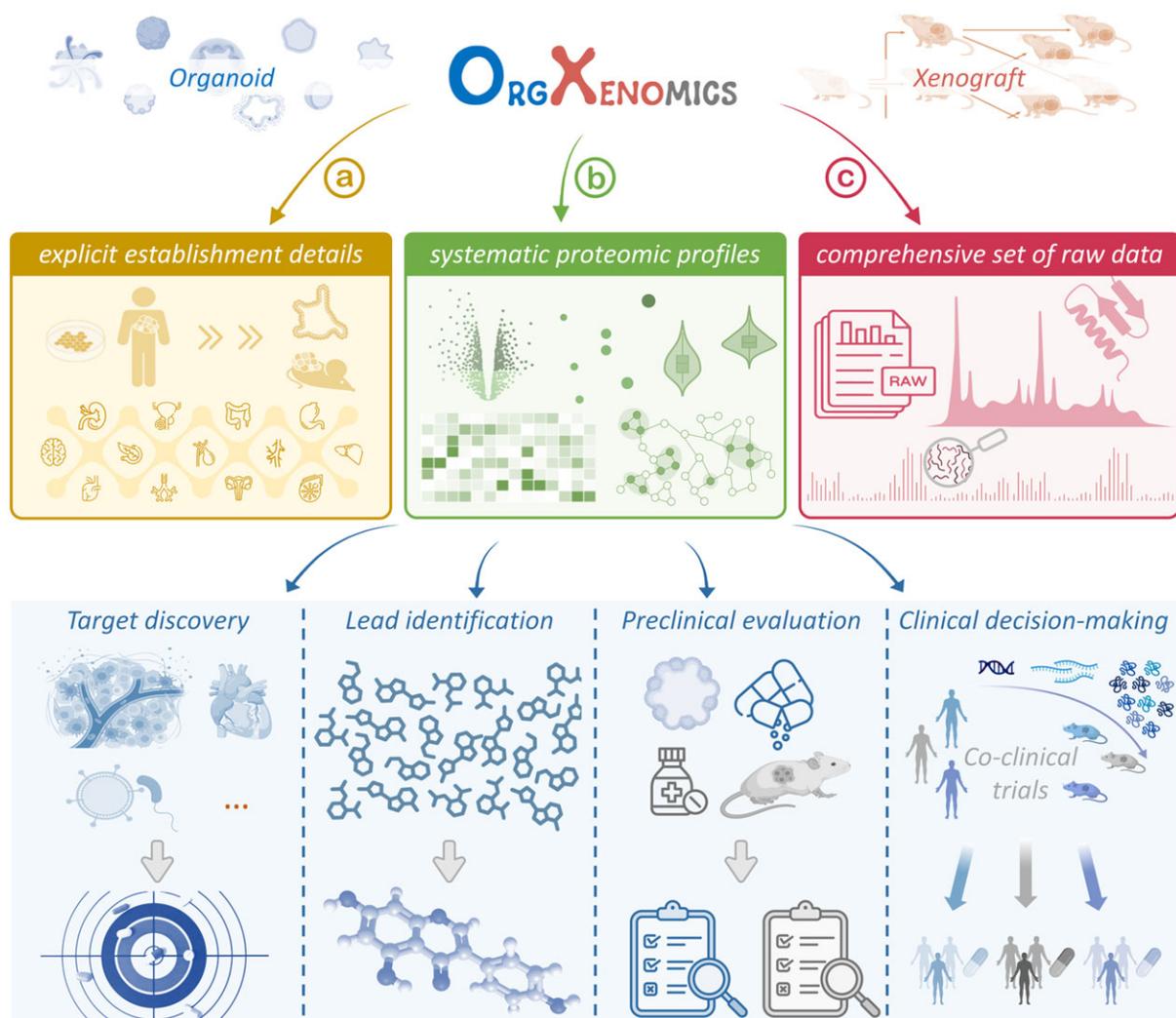
Figure 1. Three key features of *OrgXenomics* and the implications of organoid/xenograft in drug developments (including target discovery, lead identification, preclinical evaluation, and clinical decision-making, and so on). *OrgXenomics* was unique in explicitly describing the establishment details for the models of diverse tissue/organ, systematically providing proteomics profiles (such as expression, function, and interaction) for all proteins in proteomic study, and comprehensively giving the raw data for organoid/xenograft-based proteomic studies of various diseases.

approach based on the characteristics of mass spectrometry result ([50]) was applied. For example, the *K-nearest neighbor imputation* was used to replace *standard deviation-based imputation* when processing the dataset of extreme sparsity ([51]); well-performing methods, including *Box-Cox Transformation* ([52]), *Z-score Normalization* ([53]), and so on, were adopted to further strengthen the performance of data processing. *Finally*, the protein with absolute $\log_2(\mathrm{FC}) \geq 1$ and *P*-value ≤ 0.05 between two groups was identified as differentially expressed ([54,55]). For the projects with >2 groups, the differential anal-

yses between any two groups were conducted in this study. It should be noted that it was difficult for some projects to conduct differential analysis due to the absence of essential data such as the lack of sample group information.

Functional enrichment analysis and protein–protein interaction analysis

To facilitate researchers in gaining mechanistic insights into the differentially expressed proteins in each project, both
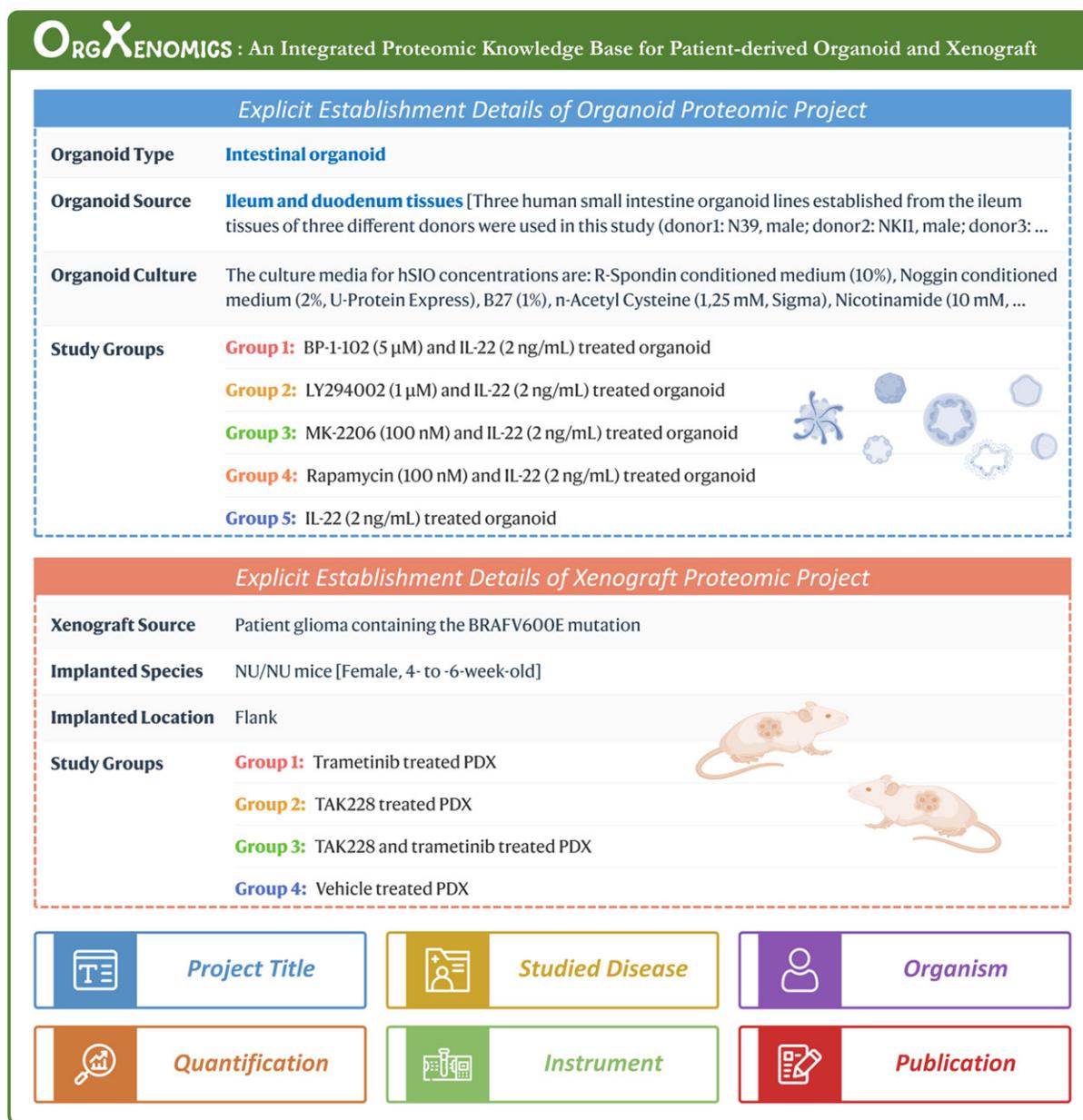
Figure 2. The explicit establishment details of organoids/xenografts proteomics projects together with their affiliated project information. For each organoid proteomics project, the *organoid type*, *organoid source* and *culture protocols* were recorded; for a studied xenograft proteomics project, the *xenograft source*, *implanted species* and *implanted location* were documented. The affiliated project information included *studied disease*, *organism*, *quantification methods*, *instrument*, etc.

functional enrichment (56–59) and protein-protein interaction (PPI) analyses (60–65) were further performed. For the functional enrichment analyses, three widely-recognized classification systems (66) were adopted in *OrgXenomics*. The organism-specific annotation files from these classification systems were downloaded as local libraries and the enrichment analysis was then conducted using *enrich* functions of *R* package *clusterProfiler* (67). Terms with *P*-values ≤0.05 were considered significantly enriched, shedding lights on the biological function and pathway associated with the identified proteins. For the PPI analyses, PPIs with confidence score ≥0.9 were collected from the STRING database (68) and the interactions among the differentially expressed proteins identified in each study were finally filtered and provided in our online database.

Interactive visualization of the proteomic profiles for proteins in each study

In our database, the proteomic profiles (expression, function, interaction, etc.) of proteins in each analysis were systematically described. As shown in Figure 3A, the expression profile of proteins was presented by diverse graphs. First, the differential expression of protein between two groups was depicted using volcano plot (69,70). In instances where more than two groups were involved, the expression profile between any two groups was depicted. The *x*-axis and *y*-axis of the volcano plot corresponded to the $\log_2(\mathrm{FC})$ and $-\log_{10}(P\text{-value})$, respectively. One dot represented a protein, and the proteins with the absolute $\log_2(\mathrm{FC}) \geq 1$ and $-\log_{10}(P\text{-value}) > 1.3$ were highlighted in RED ($\log_2(\mathrm{FC}) \geq 1$) and BLUE ($\log_2(\mathrm{FC}) \leq -1$) colors. Upon hovering the mouse over each dot, detailed

Figure 3. The proteomic profiles for all proteins in each project. (**A**) expression profiles for PDM-proteomic project. The volcano plot was provided to depict different expression levels of proteins between two groups; the heatmap was illustrated to analyze the pattern of differentially expressed proteins between two groups; the boxplot displaying the protein expressions in all studied groups was plotted to enable the direct comparison of expressions among studied groups, especially for the project of over two groups. (**B**) function and interaction profiles for PDM-proteomics projects. The bubble chart was plotted to provide top-15 most significantly enriched terms and the protein-protein interaction network described the interactions among differentially expressed proteins.

information of one protein, such as the protein and gene name, UniProt ID, $\log_2$(FC) and $-\log_{10}$(P-value) would be displayed. Second, a heatmap was also generated to facilitate the analysis of the differentially expressed proteins between two groups (71,72), and a boxplot was used to facilitate the direct comparison of protein expression across those groups, particularly in studies involving more than two groups. Boxplot could illustrate the distribution of protein expressions within each group, which enabled the reader to discern differences or similarities in protein expression levels between groups. It was important to emphasize that the volcano plots were not available for those studies that only had one single group or only had one sample in group. In such case, the heatmap and boxplot were used to display the expression of all proteins within corresponding study.

In *OrgXenomics*, the result of functional enrichment was described on the left side of Figure 3B. The top-15 most significantly enriched terms were displayed as a bubble chart,

while the complete enrichment result could be downloaded from the online database. In the bubble chart, the horizontal axis represented the enriched terms, whereas vertical axis provided the fold enrichments (defined as the ratio of the frequency of input proteins annotated for one term to that of all proteins of that term). The circle color indicated the P-value of enrichment significance with circle size reflecting the number of input proteins annotated to the corresponding term. This representation effectively encapsulated the enriched terms, the significance and the extent of protein involvement, enabling comprehensive understandings of the functional enrichment outcomes. Furthermore, the protein-protein interaction networks among differentially expressed proteins were given in *OrgXenomics* (shown on the right side of Figure 3B). The up- and down-regulated proteins were labelled using RED and BLUE color, respectively. These networks might help elucidate the potential regulatory mechanisms underlying the observed expression alterations, which give insights into the intricate
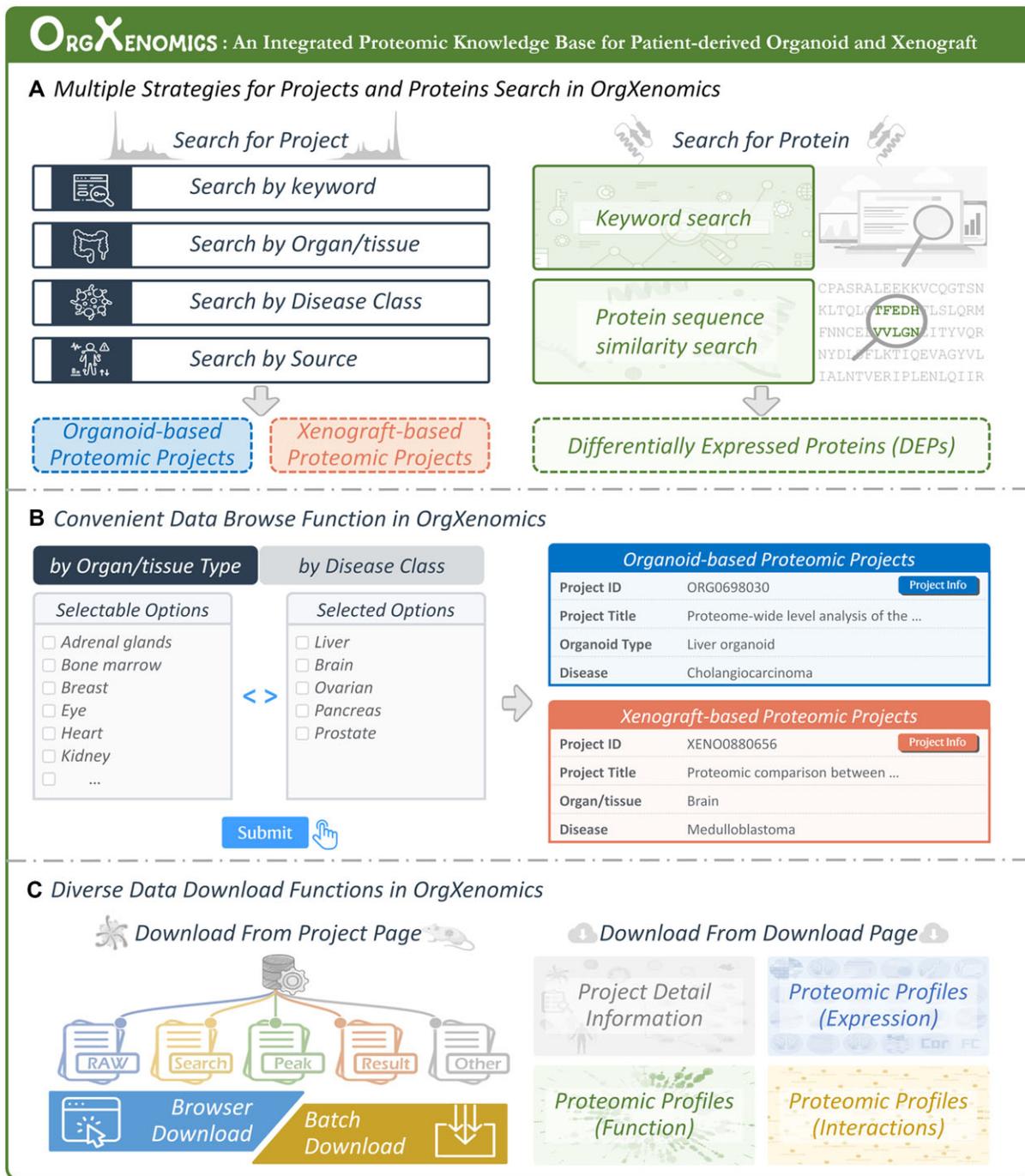
Figure 4. The functions of search, browse and download. (**A**) multiple strategies for projects and proteins search. For project search, user can use keyword search or select the option in dropdown menu. For protein search, user can input keyword or protein sequence to obtain a list of sequence-similar proteins based on the result of BLAST. (**B**) convenient browse function. Users can browse the projects based on tissue type/disease class, which helps the user to access and filter the project information. (**C**) diverse data download functions. In project page, users can download individual file using browser or download all files of a project using batch download tools. In the *Download* page, user can download the general information and proteomic profile for all projects in bulk.

interplay and functional relationships among the differentially expressed proteins.

User-friendly data search, browse and download function in OrgXenomics

OrgXenomics gave a user-friendly interface enabling the data search, visualization and download processes. As provided in

Figure 4A, *OrgXenomics* allowed user to access the projects or proteins of interest via multiple search strategies. For project search, user can use keyword search directly or utilize the dropdown menus, featuring categories such as disease class and organoid/xenograft source (shown in the left of Figure 4A). When searching for protein, users can input the keywords of protein/gene name and UniProt ID. Moreover, as described in the right of Figure 4A, user can also input protein
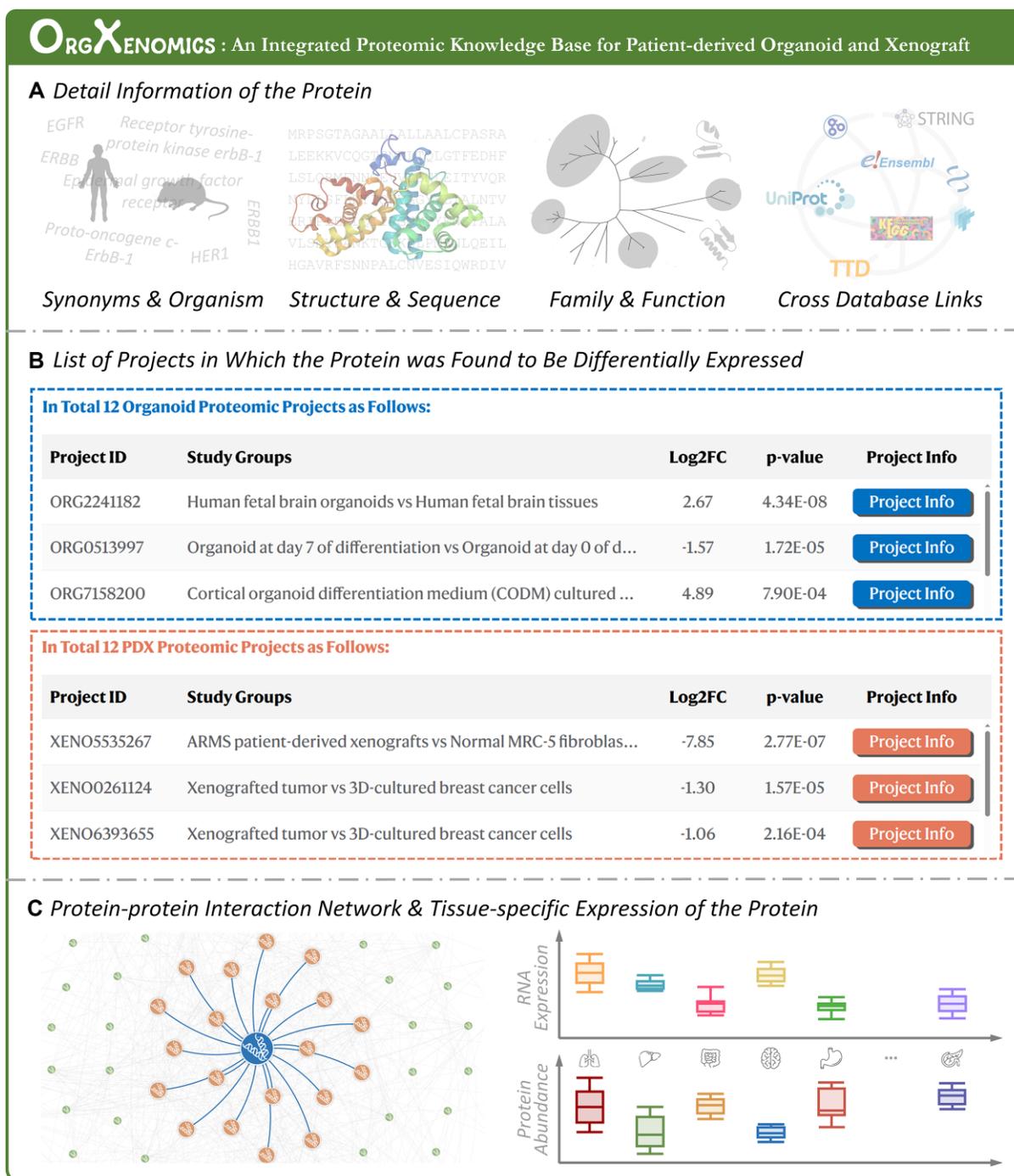
Figure 5. A typical page providing the diverse information of a protein. (**A**) basic information of each protein. A wealth of basic information for protein was provided in the upper section. (**B**) list of proteomic projects in which the protein was differentially expressed. A list of projects in which this protein was differentially expressed was accompanied with the $\log_2$(FC) and *P*-values. Users can click the button of *Project Info* to explore detailed information of corresponding projects. (**C**) PPI network and tissue-specific expression of proteins. PPI network was collected from STRING with a confidence score >0.9. The source of data for tissue-specific RNA and protein expressions level were from *Jiang*'s study (75), which quantified proteins across 32 normal human tissues.

sequences, prompting the return of a list of sequence-similar proteins based on the results generated by BLAST (73,74). Except the Project page, the protein pages (as described in Figure 5) were also constructed to offer diverse information for those proteins that were found differentially expressed in any projects collected in this database. In the upper section of the page, a wealth of detailed information of protein, in-

cluding its name, synonyms, gene names, sequence, structure, family, function, etc. (as provided in Figure 5A). In the second section of the page, the proteomic projects in which the protein was differentially expressed were listed in tabular format accompanied by the $\log_2$(FC) and *P*-value. Users can explore the detailed information of a project through clicking the '*Project Info*' button (depicted in Figure 5B). The lower
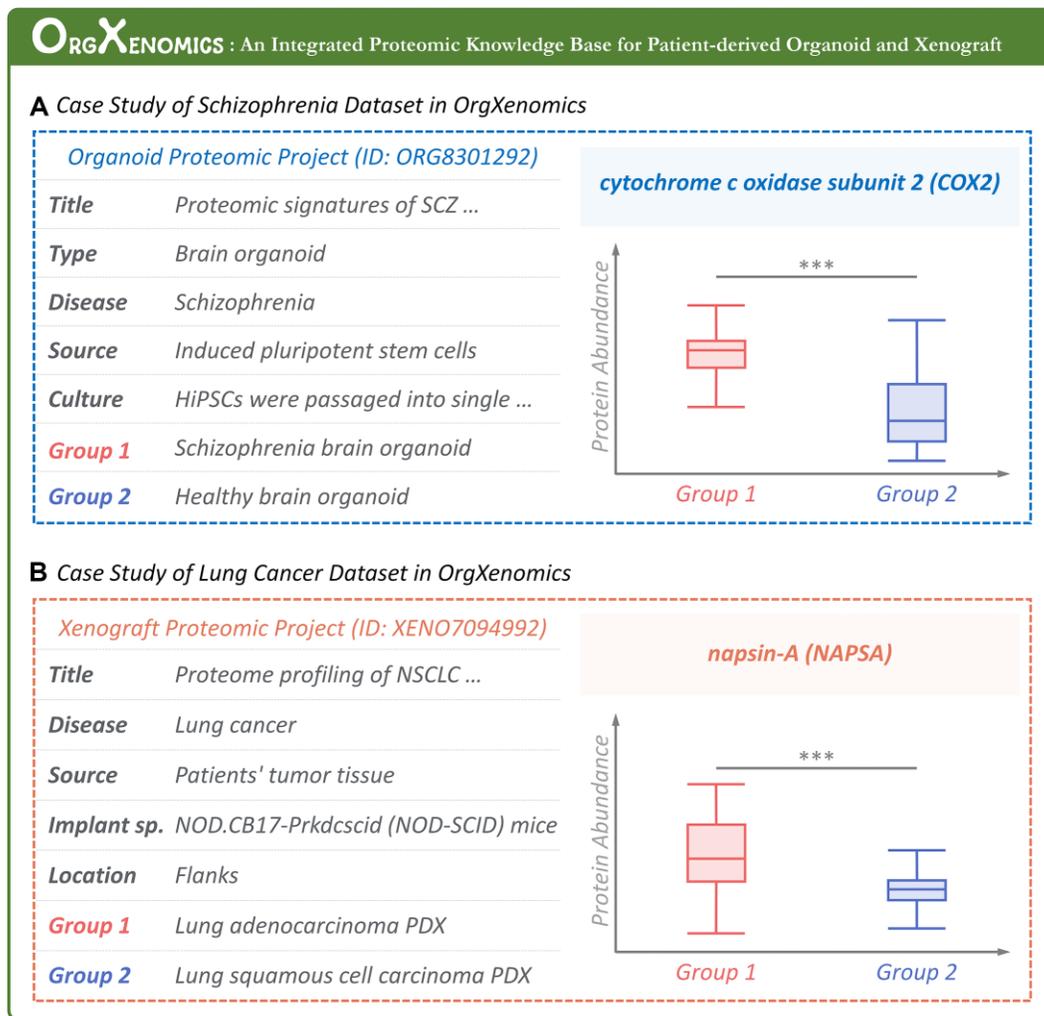
Figure 6. Case studies of organoid/xenograft proteomic datasets. (**A**) case study of *schizophrenia* dataset. The left panel described the experimental details of one organoid dataset (ORG8301292), and the right panel showed the differential expression of cytochrome c oxidase subunit 2 (COX2) identified using this organoid dataset. These reproduced the result of the previous study (76) that reported the overexpression of COX2 in the brains of *schizophrenia* patients comparing with that of healthy people. (**B**) case study of *lung cancer* dataset. The left panel provided the experimental details of one xenograft dataset (XENO7094992), while the right panel illustrated the differential expression of *napsin-A* among three PDX types (lung adenocarcinoma, large cell neuroendocrine carcinoma and lung squamous cell carcinoma). The resulting expression patterns reproduced that of previous publication (77), which reported the overexpression of *napsin-A* in the tissues of lung adenocarcinoma patients comparing with that of lung squamous cell carcinoma patients.

section of the page (shown in Figure 5C) elaborated the PPI network and the tissue-specific RNA/protein expression of any studied proteins. Particularly, PPI network was collected from STRING with a confidence score >0.9. The data for tissue-specific RNA and protein expressions were collected from *Jiang*'s study, which quantified a large number of proteins across 32 normal human tissues (75).

OrgXenomics also offered the convenient data browse function. As illustrated in Figure 4B, users can browse the projects in *OrgXenomics* by organ/tissue type or by disease class to quickly access and filter the project information. For instance, when browsing projects by tissue types (as shown in Figure 4B), user could simply select their desired organ/tissue and then the related projects of their selection would be fully listed. In addition, *OrgXenomics* also offered a variety of download functions to enhance data accessibility. On project page, user could seamlessly start the download process by clicking the 'Download' button correspond-

ing to certain file for individual download or using the download tool to batch download all files associated with certain project (as depicted on the left side of Figure 4C). Additionally, *OrgXenomics* also provided the functions of full data download (on the right side of Figure 4C). User can download the general information/proteomic profiles for all projects or the information for organ-specific studies. All such download functions collectively empowered users to effortlessly retrieve corresponding data tailored to their research objectives, thereby streamlining the data acquisition process within the *OrgXenomics*.

It was of interest to assess the consistency between the analytical results using *OrgXenomics* data and the real-world biological findings, and two case studies were shown in Figure 6. As reported, *cytochrome c oxidase subunit 2* (COX2) was found by previous analysis (76) to be overexpressed in the brains of *schizophrenia* patients comparing with that of healthy people by utilizing western blot techniques. In

this study, one organoid dataset (ORG8301292) was therefore identified from *OrgXenomics*, which described the proteomic data of brain organoids cultivated using the tissues of *schizophrenia* patients and healthy individuals. Based on the analytical results of this organoid datasets (illustrated in the right panel of Figure 6A), the overexpression of COX2 in the organoids of *schizophrenia* patients (with $\log_2(FC) = 1.35$, P-value = 0.01) was found when comparing with that of healthy individual. Such results indicated that the real-world biological findings could be successfully reproduced using the organoid proteomic data collected into *OrgXenomics*. Another case study would be the protein *napsin-A*, which was found by previous study (77) to overexpress in the tissues of *lung adenocarcinoma* patients when comparing with that of *lung squamous cell carcinoma* patients using immunohistochemistry techniques. In this study, one xenograft dataset (XENO7094992) was therefore retrieved from *OrgXenomics*, which provided the proteomic data of implanted xenografts based on the tissue of *lung adenocarcinoma* patients and *lung squamous cell carcinoma* patients. According to the analytical result of this dataset (shown in the right side of Figure 6B), the overexpression of *napsin-A* in the xenografts of *lung adenocarcinoma* patients was identified when comparing with that of *lung squamous cell carcinoma* patients (with $\log_2(FC) = 2.28$, P-value < 0.01). Such result further indicated that the real-world biological findings could be successfully reproduced based on the xenograft proteomic data provided in *OrgXenomics*.

Database construction and implementation

OrgXenomics adopted the *CentOS Linux* (v7.6.1810) as its foundational operating system, *Nginx* (v1.16.1) as the web server, and *MySQL* (v5.7.18) as database management system. The backend architecture was implemented using *Python* (v3.10.6) together with the *Django* web framework (v3.2.16). The frontend was realized using *Vue.js* (v2.6.14) enhanced with *Element UI* (v2.15.12). Additionally, the interactive visualization was enabled by *ECharts* (v.5.5.1) and *iCn3D* (v2.20.0), and the statistical analyses were performed using the *R* framework (v3.6.0). *OrgXenomics* is now accessible by all types of mainstream browsers, such as Chrome, Edge, Firefox and Safari.

Conclusion and perspectives

A database '*OrgXenomics*' was constructed here to describe the data of PDMs. It is unique in (a) describing the establishment detail for models of diverse tissues/organs, (b) providing proteomic profile (expression/function/interaction) for all expressed proteins in each study and (c) offered the raw data for organoids/xenografts-based proteomic study of different diseases. *OrgXenomics* is highly expected to server as a good complement to existing PDM databases to facilitate target discovery, lead identification, preclinical evaluation, clinical decision making, etc. To the best of our knowledge, this new database had great implication for the application of precision medicine, such as personalized drug screening (78–80), biomarker discovery (81–83), tumor heterogeneity analysis (84–86), drug resistance investigation (87–90) and combination therapy design (91–93). All these applications can contribute to more accurate patient stratification and tailored

treatment selection, thereby improving the clinical outcomes for the modern precision medications.

Data availability

OrgXenomics is a resource for analyzing and visualizing the PDM-based proteomic data and can be freely accessible without any login requirement at: https://idrblab.org/orgxenomics/

Conflict of interest statement

None declared.

References

1. Honkala,A., Malhotra,S.V., Kummar,S. and Junttila,M.R. (2022) Harnessing the predictive power of preclinical models for oncology drug development. *Nat. Rev. Drug Discov.*, **21**, 99–114.
2. Yoshida,G.J. (2020) Applications of patient-derived tumor xenograft models and tumor organoids. *J. Hematol. Oncol.*, **13**, 4.
3. Kim,J., Koo,B.K. and Knoblich,J.A. (2020) Human organoids: model systems for human biology and medicine. *Nat. Rev. Mol. Cell Biol.*, **21**, 571–584.
4. Sun,H., Cao,S., Mashl,R.J., Mo,C.K., Zaccaria,S., Wendl,M.C., Davies,S.R., Bailey,M.H., Primeau,T.M., Hoog,J., *et al.* (2021) Comprehensive characterization of 536 patient-derived xenograft models prioritizes candidatesfor targeted treatment. *Nat. Commun.*, **12**, 5086.
5. Beumer,J., Puschhof,J., Bauza-Martinez,J., Martinez-Silgado,A., Elmentaite,R., James,K.R., Ross,A., Hendriks,D., Artegiani,B., Busslinger,G.A., *et al.* (2020) High-resolution mRNA and secretome atlas of human enteroendocrine cells. *Cell*, **182**, 1062–1064.
6. Bahrami,E., Schmid,J.P., Jurinovic,V., Becker,M., Wirth,A.K., Ludwig,R., Kreissig,S., Duque Angel,T.V., Amend,D., Hunt,K.,

et al. (2023) Combined proteomics and CRISPR−Cas9 screens in PDX identify ADAM10 as essential for leukemia in vivo. *Mol. Cancer*, **22**, 107.

7. Rialdi,A., Duffy,M., Scopton,A.P., Fonseca,F., Zhao,J.N., Schwarz,M., Molina-Sanchez,P., Mzoughi,S., Arceci,E., Abril-Fornaguera,J., *et al.* (2023) WNTinib is a multi-kinase inhibitor with specificity against beta-catenin mutant hepatocellular carcinoma. *Nat Cancer*, **4**, 1157–1175.

8. Mooney,B., Negri,G.L., Shyp,T., Delaidelli,A., Zhang,H.F., Spencer Miko,S.E., Weiner,A.K., Radaoui,A.B., Shraim,R., Lizardo,M.M., *et al.* (2024) Surface and global proteome analyses identify ENPP1 and other surface proteins as actionable immunotherapeutic targets in Ewing sarcoma. *Clin. Cancer Res.*, **30**, 1022–1037.

9. Hendriks,D., Brouwers,J.F., Hamer,K., Geurts,M.H., Luciana,L., Massalini,S., Lopez-Iglesias,C., Peters,P.J., Rodriguez-Colman,M.J., Chuva de Sousa Lopes,S., *et al.* (2023) Engineered human hepatocyte organoids enable CRISPR-based target discovery and drug screening for steatosis. *Nat. Biotechnol.*, **41**, 1567–1581.

10. Li,Y.H., Li,X.X., Hong,J.J., Wang,Y.X., Fu,J.B., Yang,H., Yu,C.Y., Li,F.C., Hu,J., Xue,W.W., *et al.* (2020) Clinical trials, progression-speed differentiating features and swiftness rule of the innovative targets of first-in-class drugs. *Brief. Bioinform.*, **21**, 649–662.

11. Krstic,J., Reinisch,I., Schindlmaier,K., Galhuber,M., Riahi,Z., Berger,N., Kupper,N., Moyschewitz,E., Auer,M., Michenthaler,H., *et al.* (2022) Fasting improves therapeutic response in hepatocellular carcinoma through p53-dependent metabolic synergism. *Sci. Adv.*, **8**, eabh2635.

12. Li,F., Yin,J., Lu,M., Mou,M., Li,Z., Zeng,Z., Tan,Y., Wang,S., Chu,X., Dai,H., *et al.* (2023) DrugMAP: molecular atlas and pharma-information of all drugs. *Nucleic Acids Res.*, **51**, D1288–D1299.

13. Xue,W., Fu,T., Deng,S., Yang,F., Yang,J. and Zhu,F. (2022) Molecular mechanism for the allosteric inhibition of the human serotonin transporter by antidepressant escitalopram. *ACS Chem. Neurosci.*, **13**, 340–351.

14. Franciosa,G., Smits,J.G.A., Minuzzo,S., Martinez-Val,A., Indraccolo,S. and Olsen,J.V. (2021) Proteomics of resistance to Notch1 inhibition in acute lymphoblastic leukemia reveals targetable kinase signatures. *Nat. Commun.*, **12**, 2507.

15. Wang,J., Yu,H., Dong,W., Zhang,C., Hu,M., Ma,W., Jiang,X., Li,H., Yang,P. and Xiang,D. (2023) N6-methyladenosine-mediated up-regulation of FZD10 regulates liver cancer stem cells' properties and lenvatinib resistance through WNT/beta-catenin and hippo signaling pathways. *Gastroenterology*, **164**, 990–1005.

16. Sun,X., Zhang,Y., Li,H., Zhou,Y., Shi,S., Chen,Z., He,X., Zhang,H., Li,F., Yin,J., *et al.* (2023) DRESIS: the first comprehensive landscape of drug resistance information. *Nucleic Acids Res.*, **51**, D1263–D1275.

17. Shen,L., Sun,X., Chen,Z., Guo,Y., Shen,Z., Song,Y., Xin,W., Ding,H., Ma,X., Xu,W., *et al.* (2024) ADCdb: the database of antibody-drug conjugates. *Nucleic Acids Res.*, **52**, D1097–D1109.

18. Lu,M.K., Yin,J.Y., Zhu,Q., Lin,G.L., Mou,M.J., Liu,F.Y., Pan,Z.Q., You,N.X., Lian,X.C., Li,F.C., *et al.* (2023) Artificial intelligence in pharmaceutical sciences. *Engineering.*, **27**, 37–69.

19. Zheng,L., Shi,S., Lu,M., Fang,P., Pan,Z., Zhang,H., Zhou,Z., Zhang,H., Mou,M., Huang,S., *et al.* (2024) AnnoPRO: a strategy for protein function annotation based on multi-scale protein representation and a hybrid deep learning of dual-path encoding. *Genome Biol.*, **25**, 41.

20. Wang,Y., Chen,Z., Pan,Z., Huang,S., Liu,J., Xia,W., Zhang,H., Zheng,M., Li,H., Hou,T., *et al.* (2023) RNAincoder: a deep learning-based encoder for RNA and RNA-associated interaction. *Nucleic Acids Res.*, **51**, W509–W519.

21. Karkampouna,S., La Manna,F., Benjak,A., Kiener,M., De Menna,M., Zoni,E., Grosjean,J., Klima,I., Garofoli,A., Bolis,M., *et al.* (2021) Patient-derived xenografts and organoids model therapy response in prostate cancer. *Nat. Commun.*, **12**, 1117.

22. van de Merbel,A.F., van der Horst,G. and van der Pluijm,G. (2021) Patient-derived tumour models for personalized therapeutics in urological cancers. *Nat. Rev. Urol.*, **18**, 33–45.

23. Vlachogiannis,G., Hedayat,S., Vatsiou,A., Jamin,Y., Fernandez-Mateos,J., Khan,K., Lampis,A., Eason,K., Huntingford,I., Burke,R., *et al.* (2018) Patient-derived organoids model treatment response of metastatic gastrointestinal cancers. *Science*, **359**, 920–926.

24. Wang,Y., Pan,Z., Mou,M., Xia,W., Zhang,H., Zhang,H., Liu,J., Zheng,L., Luo,Y., Zheng,H., *et al.* (2023) A task-specific encoding algorithm for RNAs and RNA-associated interactions based on convolutional autoencoder. *Nucleic Acids Res.*, **51**, e110.

25. Perez-Riverol,Y., Bai,J., Bandla,C., Garcia-Seisdedos,D., Hewapathirana,S., Kamatchinathan,S., Kundu,D.J., Prakash,A., Frericks-Zipper,A., Eisenacher,M., *et al.* (2022) The PRIDE database resources in 2022: a hub for mass spectrometry-based proteomics evidences. *Nucleic Acids Res.*, **50**, D543–D552.

26. Moriya,Y., Kawano,S., Okuda,S., Watanabe,Y., Matsumoto,M., Takami,T., Kobayashi,D., Yamanouchi,Y., Araki,N., Yoshizawa,A.C., *et al.* (2019) The jPOST environment: an integrated proteomics data repository and database. *Nucleic Acids Res.*, **47**, D1218–D1224.

27. Choi,M., Carver,J., Chiva,C., Tzouros,M., Huang,T., Tsai,T.H., Pullman,B., Bernhardt,O.M., Huttenhain,R., Teo,G.C., *et al.* (2020) MassIVE.Quant: a community resource of quantitative mass spectrometry-based proteomics datasets. *Nat. Methods*, **17**, 981–984.

28. Chen,T., Ma,J., Liu,Y., Chen,Z., Xiao,N., Lu,Y., Fu,Y., Yang,C., Li,M., Wu,S., *et al.* (2022) iProX in 2021: connecting proteomics data sharing with big data. *Nucleic Acids Res.*, **50**, D1522–D1527.

29. Deutsch,E.W., Bandeira,N., Perez-Riverol,Y., Sharma,V., Carver,J.J., Mendoza,L., Kundu,D.J., Wang,S., Bandla,C., Kamatchinathan,S., *et al.* (2023) The ProteomeXchange consortium at 10 years: 2023 update. *Nucleic Acids Res.*, **51**, D1539–D1548.

30. UniProt, C. (2023) UniProt: the universal protein knowledgebase in 2023. *Nucleic Acids Res.*, **51**, D523–D531.

31. Burley,S.K., Bhikadiya,C., Bi,C., Bittrich,S., Chao,H., Chen,L., Craig,P.A., Crichlow,G.V., Dalenberg,K., Duarte,J.M., *et al.* (2023) RCSB Protein Data Bank (RCSB.org): delivery of experimentally-determined PDB structures alongside one million computed structure models of proteins from artificial intelligence/machine learning. *Nucleic Acids Res.*, **51**, D488–D508.

32. Varadi,M., Bertoni,D., Magana,P., Paramval,U., Pidruchna,I., Radhakrishnan,M., Tsenkov,M., Nair,S., Mirdita,M., Yeo,J., *et al.* (2024) AlphaFold protein structure database in 2024: providing structure coverage for over 214 million protein sequences. *Nucleic Acids Res.*, **52**, D368–D375.

33. Zhou,Y., Zhang,Y., Zhao,D., Yu,X., Shen,X., Zhou,Y., Wang,S., Qiu,Y., Chen,Y. and Zhu,F. (2024) TTD: therapeutic target database describing target druggability information. *Nucleic Acids Res.*, **52**, D1465–D1477.

34. Schoch,C.L., Ciufo,S., Domrachev,M., Hotton,C.L., Kannan,S., Khovanskaya,R., Leipe,D., McVeigh,R., O'Neill,K., Robbertse,B., *et al.* (2020) NCBI Taxonomy: a comprehensive update on curation, resources and tools. *Database*, **2020**, baaa062.

35. Haft,D.H., Badretdin,A., Coulouris,G., DiCuccio,M., Durkin,A.S., Jovenitti,E., Li,W., Mersha,M., O'Neill,K.R., Virothaisakun,J., *et al.* (2024) RefSeq and the prokaryotic genome annotation pipeline in the age of metagenomes. *Nucleic Acids Res.*, **52**, D762–D769.

36. Harrison,P.W., Amode,M.R., Austine-Orimoloye,O., Azov,A.G., Barba,M., Barnes,I., Becker,A., Bennett,R., Berry,A., Bhai,J., *et al.* (2024) Ensembl 2024. *Nucleic Acids Res.*, **52**, D891–D899.

37. Yin,J., Sun,W., Li,F., Hong,J., Li,X., Zhou,Y., Lu,Y., Liu,M., Zhang,X., Chen,N., *et al.* (2020) VARIDT 1.0: variability of drug transporter database. *Nucleic Acids Res.*, **48**, D1042–D1050.

38. Kanehisa,M., Furumichi,M., Sato,Y., Kawashima,M. and Ishiguro-Watanabe,M. (2023) KEGG for taxonomy-based analysis of pathways and genomes. *Nucleic Acids Res.*, **51**, D587–D592.

39. Milacic,M., Beavers,D., Conley,P., Gong,C., Gillespie,M., Griss,J., Haw,R., Jassal,B., Matthews,L., May,B., *et al.* (2024) The reactome pathway knowledgebase 2024. *Nucleic Acids Res.*, **52**, D672–D678.

40. Aleksander,S.A., Balhoff,J., Carbon,S., Cherry,J.M., Drabkin,H.J., Ebert,D., Feuermann,M., Gaudet,P., Harris,N.L., Hill,D.P., *et al.* (2023) The gene ontology knowledgebase in 2023. *Genetics*, **224**, iyad031.

41. Lancet,T. (2018) ICD-11: a brave attempt at classifying a new world. *Lancet*, **391**, 2476.

42. Zhang,Y., Zhou,Y., Zhou,Y., Yu,X., Shen,X., Hong,Y., Zhang,Y., Wang,S., Mou,M., Zhang,J., *et al.* (2024) TheMarker: a comprehensive database of therapeutic biomarkers. *Nucleic Acids Res.*, **52**, D1450–D1464.

43. Bruford,E.A., Braschi,B., Denny,P., Jones,T.E.M., Seal,R.L. and Tweedie,S. (2020) Guidelines for human gene nomenclature. *Nat. Genet.*, **52**, 754–758.

44. Yin,J., Li,F., Zhou,Y., Mou,M., Lu,Y., Chen,K., Xue,J., Luo,Y., Fu,J., He,X., *et al.* (2021) INTEDE: interactome of drug-metabolizing enzymes. *Nucleic Acids Res.*, **49**, D1233–D1243.

45. Ma,Q., Tao,H., Li,Q., Zhai,Z., Zhang,X., Lin,Z., Kuang,N. and Pan,J. (2023) OrganoidDB: a comprehensive organoid database for the multi-perspective exploration of bulk and single-cell transcriptomic profiles of organoids. *Nucleic Acids Res.*, **51**, D1086–D1093.

46. Sayers,E.W., Beck,J., Bolton,E.E., Brister,J.R., Chan,J., Comeau,D.C., Connor,R., DiCuccio,M., Farrell,C.M., Feldgarden,M., *et al.* (2024) Database resources of the national center for biotechnology information. *Nucleic Acids Res.*, **52**, D33–D43.

47. Sinitcyn,P., Hamzeiy,H., Salinas Soto,F., Itzhak,D., McCarthy,F., Wichmann,C., Steger,M., Ohmayer,U., Distler,U., Kaspar-Schoenefeld,S., *et al.* (2021) MaxDIA enables library-based and library-free data-independent acquisition proteomics. *Nat. Biotechnol.*, **39**, 1563–1573.

48. Tyanova,S., Temu,T., Sinitcyn,P., Carlson,A., Hein,M.Y., Geiger,T., Mann,M. and Cox,J. (2016) The perseus computational platform for comprehensive analysis of (prote)omics data. *Nat. Methods*, **13**, 731–740.

49. Tang,J., Fu,J., Wang,Y., Li,B., Li,Y., Yang,Q., Cui,X., Hong,J., Li,X., Chen,Y., *et al.* (2020) ANPELA: analysis and performance assessment of the label-free quantification workflow for metaproteomic studies. *Brief. Bioinform.*, **21**, 621–636.

50. Li,B., Tang,J., Yang,Q., Li,S., Cui,X., Li,Y., Chen,Y., Xue,W., Li,X. and Zhu,F. (2017) NOREVA: normalization and evaluation of MS-based metabolomics data. *Nucleic Acids Res.*, **45**, W162–W170.

51. Li,F., Zhou,Y., Zhang,Y., Yin,J., Qiu,Y., Gao,J. and Zhu,F. (2022) POSREG: proteomic signature discovered by simultaneously optimizing its reproducibility and generalizability. *Brief. Bioinform.*, **23**, bbac040.

52. Fu,J., Zhang,Y., Wang,Y., Zhang,H., Liu,J., Tang,J., Yang,Q., Sun,H., Qiu,W., Ma,Y., *et al.* (2022) Optimization of metabolomic data processing using NOREVA. *Nat. Protoc.*, **17**, 129–151.

53. Carvalho,L.B., Teigas-Campos,P.A.D., Jorge,S., Protti,M., Mercolini,L., Dhir,R., Wisniewski,J.R., Lodeiro,C., Santos,H.M. and Capelo,J.L. (2024) Normalization methods in mass spectrometry-based analytical proteomics: a case study based on renal cell carcinoma datasets. *Talanta*, **266**, 124953.

54. Li,L., Wei,Y., To,C., Zhu,C.Q., Tong,J., Pham,N.A., Taylor,P., Ignatchenko,V., Ignatchenko,A., Zhang,W., *et al.* (2014) Integrated omic analysis of lung cancer reveals metabolism proteome signatures with prognostic impact. *Nat. Commun.*, **5**, 5469.

55. Lian,X., Zhang,Y., Zhou,Y., Sun,X., Huang,S., Dai,H., Han,L. and Zhu,F. (2024) SingPro: a knowledge base providing single-cell proteomic data. *Nucleic Acids Res.*, **52**, D552–D561.

56. Liu,H., Yuan,M., Mitra,R., Zhou,X., Long,M., Lei,W., Zhou,S., Huang,Y.E., Hou,F., Eischen,C.M., *et al.* (2022) CTpathway: a

57. Reimand,J., Isserlin,R., Voisin,V., Kucera,M., Tannus-Lopes,C., Rostamianfar,A., Wadi,L., Meyer,M., Wong,J., Xu,C., *et al.* (2019) Pathway enrichment analysis and visualization of omics data using g:profiler, GSEA, cytoscape and enrichmentmap. *Nat. Protoc.*, **14**, 482–517.

58. Yang,Q., Li,B., Chen,S., Tang,J., Li,Y., Li,Y., Zhang,S., Shi,C., Zhang,Y., Mou,M., *et al.* (2021) MMEASE: online meta-analysis of metabolomic data by enhanced metabolite annotation, marker selection and enrichment analysis. *J. Proteomics*, **232**, 104023.

59. Yang,Q., Wang,Y., Zhang,Y., Li,F., Xia,W., Zhou,Y., Qiu,Y., Li,H. and Zhu,F. (2020) NOREVA: enhanced normalization and evaluation of time-course and multi-class metabolomic data. *Nucleic Acids Res.*, **48**, W436–W448.

60. Huttlin,E.L., Bruckner,R.J., Navarrete-Perea,J., Cannon,J.R., Baltier,K., Gebreab,F., Gygi,M.P., Thornock,A., Zarraga,G., Tam,S., *et al.* (2021) Dual proteome-scale networks reveal cell-specific remodeling of the human interactome. *Cell*, **184**, 3022–3040.

61. Liu,Z.P. and Chen,L. (2012) Proteome-wide prediction of protein-protein interactions from high-throughput data. *Protein Cell*, **3**, 508–520.

62. Tomkins,J.E. and Manzoni,C. (2021) Advances in protein-protein interaction network analysis for Parkinson's disease. *Neurobiol. Dis.*, **155**, 105391.

63. Mou,M., Pan,Z., Zhou,Z., Zheng,L., Zhang,H., Shi,S., Li,F., Sun,X. and Zhu,F. (2023) A transformer-based ensemble framework for the prediction of protein-protein interaction sites. *Research (Wash D C).*, **6**, 0240.

64. Zhang,S., Amahong,K., Zhang,C., Li,F., Gao,J., Qiu,Y. and Zhu,F. (2022) RNA-RNA interactions between SARS-CoV-2 and host benefit viral development and evolution during COVID-19 infection. *Brief Bioinform*, **23**, bbab397.

65. Xue,W., Yang,F., Wang,P., Zheng,G., Chen,Y., Yao,X. and Zhu,F. (2018) What contributes to serotonin-norepinephrine reuptake inhibitors' dual-targeting mechanism? The key role of transmembrane domain 6 in human serotonin and norepinephrine transporters revealed by molecular dynamics simulation. *ACS Chem. Neurosci.*, **9**, 1128–1140.

66. Yang,Q., Li,B., Tang,J., Cui,X., Wang,Y., Li,X., Hu,J., Chen,Y., Xue,W., Lou,Y., *et al.* (2020) Consistent gene signature of schizophrenia identified by a novel feature selection strategy from comprehensive sets of transcriptomic data. *Brief Bioinform*, **21**, 1058–1068.

67. Wu,T., Hu,E., Xu,S., Chen,M., Guo,P., Dai,Z., Feng,T., Zhou,L., Tang,W., Zhan,L., *et al.* (2021) clusterProfiler 4.0: a universal enrichment tool for interpreting omics data. *Innovation.*, **2**, 100141.

68. Szklarczyk,D., Kirsch,R., Koutrouli,M., Nastou,K., Mehryary,F., Hachilif,R., Gable,A.L., Fang,T., Doncheva,N.T., Pyysalo,S., *et al.* (2023) The STRING database in 2023: protein-protein association networks and functional enrichment analyses for any sequenced genome of interest. *Nucleic Acids Res.*, **51**, D638–D646.

69. Mullan,K.A., Bramberger,L.M., Munday,P.R., Goncalves,G., Revote,J., Mifsud,N.A., Illing,P.T., Anderson,A., Kwan,P., Purcell,A.W., *et al.* (2021) ggVolcanoR: a shiny app for customizable visualization of differential expression datasets. *Comput. Struct. Biotechnol. J.*, **19**, 5735–5740.

70. Song,J., Jiang,J., Kuai,L., Luo,Y., Xing,M., Luo,Y., Ru,Y., Sun,X., Zhang,H., Liu,T., *et al.* (2022) TMT-based proteomics analysis reveals the protective effect of Jueyin granules on imiquimod-induced psoriasis mouse model by causing autophagy. *Phytomedicine*, **96**, 153846.

71. Ning,W., Wei,Y., Gao,L., Han,C., Gou,Y., Fu,S., Liu,D., Zhang,C., Huang,X., Wu,S., *et al.* (2022) HemI 2.0: an online service for heatmap illustration. *Nucleic Acids Res.*, **50**, W405–W411.

72. Ji,Z., Chen,S., Cui,J., Huang,W., Zhang,R., Wei,J. and Zhang,S. (2021) OCT4-dependent FoxC1 activation improves the survival

cross talk-based pathway enrichment analysis method for cancer research. *Genome Med*, **14**, 118.

and neovascularization of mesenchymal stem cells under myocardial ischemia. *Stem Cell Res. Ther.*, **12**, 483.

73. Boratyn,G.M., Camacho,C., Cooper,P.S., Coulouris,G., Fong,A., Ma,N., Madden,T.L., Matten,W.T., McGinnis,S.D., Merezhuk,Y., *et al.* (2013) BLAST: a more efficient report with usability improvements. *Nucleic Acids Res.*, **41**, W29–W33.

74. Zielezinski,A., Barylski,J. and Karlowski,W.M. (2021) Taxonomy-aware, sequence similarity ranking reliably predicts phage-host relationships. *BMC Biol.*, **19**, 223.

75. Jiang,L., Wang,M., Lin,S., Jian,R., Li,X., Chan,J., Dong,G., Fang,H., Robinson,A.E., Consortium,G.T., *et al.* (2020) A quantitative proteome map of the human body. *Cell*, **183**, 269–283.

76. MacDowell,K.S., Pinacho,R., Leza,J.C., Costa,J., Ramos,B. and Garcia-Bueno,B. (2017) Differential regulation of the TLR4 signalling pathway in post-mortem prefrontal cortex and cerebellum in chronic schizophrenia: relationship with SP transcription factors. *Prog. Neuropsychopharmacol. Biol. Psychiatry*, **79**, 481–492.

77. Kai,Y., Amatya,V.J., Kushitani,K., Kambara,T., Suzuki,R., Fujii,Y., Tsutani,Y., Miyata,Y., Okada,M. and Takeshima,Y. (2021) Glypican-1 is a novel immunohistochemical marker to differentiate poorly differentiated squamous cell carcinoma from solid predominant adenocarcinoma of the lung. *Transl. Lung Cancer Res.*, **10**, 766–775.

78. Guillen,K.P., Fujita,M., Butterfield,A.J., Scherer,S.D., Bailey,M.H., Chu,Z., DeRose,Y.S., Zhao,L., Cortes-Sanchez,E., Yang,C.H., *et al.* (2022) A human breast cancer-derived xenograft and organoid platform for drug discovery and precision oncology. *Nat. Cancer*, **3**, 232–250.

79. Broutier,L., Mastrogiovanni,G., Verstegen,M.M., Francies,H.E., Gavarro,L.M., Bradshaw,C.R., Allen,G.E., Arnes-Benito,R., Sidorova,O., Gaspersz,M.P., *et al.* (2017) Human primary liver cancer-derived organoid cultures for disease modeling and drug screening. *Nat. Med.*, **23**, 1424–1435.

80. Han,Y., Duan,X., Yang,L., Nilsson-Payant,B.E., Wang,P., Duan,F., Tang,X., Yaron,T.M., Zhang,T., Uhl,S., *et al.* (2021) Identification of SARS-CoV-2 inhibitors using lung and colonic organoids. *Nature*, **589**, 270–275.

81. Lasse,M., El Saghir,J., Berthier,C.C., Eddy,S., Fischer,M., Laufer,S.D., Kylies,D., Hutzfeldt,A., Bonin,L.L., Dumoulin,B., *et al.* (2023) An integrated organoid omics map extends modeling potential of kidney disease. *Nat. Commun.*, **14**, 4903.

82. Jiang,L., Qin,J., Dai,Y., Zhao,S., Zhan,Q., Cui,P., Ren,L., Wang,X., Zhang,R., Gao,C., *et al.* (2024) Prospective observational study

83. Ji,S., Feng,L., Fu,Z., Wu,G., Wu,Y., Lin,Y., Lu,D., Song,Y., Cui,P., Yang,Z., *et al.* (2023) Pharmaco-proteogenomic characterization of liver cancer organoids for precision oncology. *Sci. Transl. Med.*, **15**, eadg3358.

84. Kopper,O., de Witte,C.J., Lohmussaar,K., Valle-Inclan,J.E., Hami,N., Kester,L., Balgobind,A.V., Korving,J., Proost,N., Begthel,H., *et al.* (2019) An organoid platform for ovarian cancer captures intra- and interpatient heterogeneity. *Nat. Med.*, **25**, 838–849.

85. Jacob,F., Salinas,R.D., Zhang,D.Y., Nguyen,P.T.T., Schnoll,J.G., Wong,S.Z.H., Thokala,R., Sheikh,S., Saxena,D., Prokop,S., *et al.* (2020) A patient-derived glioblastoma organoid model and biobank recapitulates inter- and intra-tumoral heterogeneity. *Cell*, **180**, 188–204.

86. Xu,H., Jiao,D., Liu,A. and Wu,K. (2022) Tumor organoids: applications in cancer modeling and potentials in precision medicine. *J. Hematol. Oncol.*, **15**, 58.

87. Zhang,Z., Karthaus,W.R., Lee,Y.S., Gao,V.R., Wu,C., Russo,J.W., Liu,M., Mota,J.M., Abida,W., Linton,E., *et al.* (2020) Tumor microenvironment-derived NRG1 promotes antiandrogen resistance in prostate cancer. *Cancer Cell*, **38**, 279–296.

88. Sun,Y., Revach,O.Y., Anderson,S., Kessler,E.A., Wolfe,C.H., Jenney,A., Mills,C.E., Robitschek,E.J., Davis,T.G.R., Kim,S., *et al.* (2023) Targeting TBK1 to overcome resistance to cancer immunotherapy. *Nature*, **615**, 158–167.

89. Shu,S., Lin,C.Y., He,H.H., Witwicki,R.M., Tabassum,D.P., Roberts,J.M., Janiszewska,M., Huh,S.J., Liang,Y., Ryan,J., *et al.* (2016) Response and resistance to BET bromodomain inhibitors in triple-negative breast cancer. *Nature*, **529**, 413–417.

90. Nicolas,A.M., Pesic,M., Engel,E., Ziegler,P.K., Diefenhardt,M., Kennel,K.B., Buettner,F., Conche,C., Petrocelli,V., Elwakeel,E., *et al.* (2022) Inflammatory fibroblasts mediate resistance to neoadjuvant therapy in rectal cancer. *Cancer Cell*, **40**, 168–184.

91. Letai,A., Bhola,P. and Welm,A.L. (2022) Functional precision oncology: testing tumors with drugs to identify vulnerabilities and novel combinations. *Cancer Cell*, **40**, 26–35.

92. Koikawa,K., Kibe,S., Suizu,F., Sekino,N., Kim,N., Manz,T.D., Pinch,B.J., Akshinthala,D., Verma,A., Gaglia,G., *et al.* (2021) Targeting Pin1 renders pancreatic cancer eradicable by synergizing with immunochemotherapy. *Cell*, **184**, 4753–4771.

93. Driehuis,E., Kolders,S., Spelier,S., Lohmussaar,K., Willems,S.M., Devriese,L.A., de Bree,R., de Ruiter,E.J., Korving,J., Begthel,H., *et al.* (2019) Oral mucosal organoids as a potential platform for personalized cancer therapy. *Cancer Discov.*, **9**, 852–871.